Reentrant ordering transition of asymmetric copolymer solution film confined between polymer-grafted surfaces

Chun-lai Ren and Yu-qiang Ma*
National Laboratory of Solid State Microstructures, Nanjing University, Nanjing 210093, China
(Received 22 February 2005; revised manuscript received 21 September 2005; published 2 November 2005)

We study the equilibrium morphology of an asymmetric *A*-*B* diblock copolymer solution film confined between homopolymer-grafted substrates by using self-consistent-field calculations. We find that on decreasing the copolymer concentration, a reentrant structural transformation between hexagonal→lamellar →hexagonal phases occurs as a result of the competition between the wetting effect of the brush surface and the bulk phase behavior of the asymmetric copolymer driven by the *A*-*B* interfacial tension.

DOI: 10.1103/PhysRevE.72.051804 PACS number(s): 61.25.Hq, 68.55.−a, 81.07.−b

Block copolymers have received much attention, both experimentally and theoretically, because they can microphase separate to form a wide range of highly ordered nanoscale morphpologies [1] which help to design new functional materials. Depending on the relative fraction of block components, the self-assembled regular structures can be lamellar, cylindrical, and spherical. Recently, there has been a growing amount of studies on the ordering behavior of films of block copolymers. Several methods have been developed for realizing the well-defined structures, including confinement [2–11], external fields [12,13], solvent field [14,15], patterned surfaces [16,17], and surface topography [18,19]. In particular, surface effects play a very important role in the phase separation of films, which can change bulk phase behavior of copolymers. For example, a symmetric block copolymer film with comparable thickness to the bulk domain [6,8], which is confined between two solid surfaces, can often form a lamellar phase. The orientation of the formed lamellae is either parallel or perpendicular to the substrates, which strongly depends on the film thickness and wetting property of the confining surfaces [3,20–25].

Furthermore, if one considers copolymer solutions, the phase behavior will become more complicated due to the diluting effects from solvents. Previous theoretical studies have found order-order and order-disorder transitions of block copolymer solutions [26–28] and examined the possible macrophase separation and regions of two-phase coexistence [29,30] as functions of solvent selectivity, temperature, and the concentration and relative composition of copolymers. Experimental studies have also demonstrated such rich phase transitons [31,32]. In contrast to pure copolymer film, however, the phase behavior of copolymer solution films has received much less attention. In the present paper, we present a theoretical study on asymmetric diblock copolymer solution films confined between two surfaces by using self-consistent-field theory (SCFT) [33] and find that a rich phase behavior of well-defined highly ordered structures can be achieved by grafting polymer chains onto surfaces. As is well known, the polymer chains, which are grafted by one end to a solid surface at relatively high concentrations, stretch away from the interface, forming a polymer "brush" [34]. Polymer brushes can modify surface properties including adhesion, lubrication, and wetting behavior [35], which have many useful applications such as colloidal stabilization, polymeric surfactant, and biocompatibility. Here, we will give emphasis to different entropy repulsive effects of polymer brushes to long copolymer chains and small solvent molecules, which can control the thickness of confined solution film. The aim is to consider the influences of entropically elastic effects of brushes on the asymmetric copolymer phase-separating behavior [36]. By calculating the equilibrium morphology of asymmetric diblock copolymer solution films, we find a reentrant hexagonal-lamellar-hexagonal transition upon variation of the solution concentration. The effect may be attributed to the competition among the wetting interfaces of brushes, the asymmetric copolymer bulk phase behavior, and the effective thickness of confined films.

We consider a mixture of *A*-*B*-diblock copolymers and solvent confined between two planar surfaces with a distance L_z along the z axis. The two substrates which are grafted with n_{br} *A*-type homopolymer chains are horizontally placed in xy plane and positioned at $z=0$ and $z=L_z$, respectively. We assume translational invariance along the y axis, and then the calculation can be reduced to the xz plane. The copolymer concentration is ψ_{co} with the fraction f_A of *A* segments. All polymer chains are flexible with the same polymerization N and statistical length a, and incompressible with a segment volume ρ_0^{-1}. The volume of the system V is $L_x \times L_z$, where L_x is the lateral length of the surfaces along the x axis. The grafting density is defined as $\sigma=n_{br}/2L_x$; the average volume fraction of grafted chains is $\bar{\varphi}_{br}=n_{br}N\rho_0^{-1}/V$, the copolymer $\bar{\varphi}_{co}=n_{co}N\rho_0^{-1}/V=(V-n_{br}N\rho_0^{-1})\psi_{co}/V$ where ψ_{co} is the copolymer solution concentration, and the solvent $\bar{\varphi}_s=1-\bar{\varphi}_{br}-\bar{\varphi}_{co}$.

In the SCFT theory, the free energy F for the present system is given by

*Author to whom correspondence should be addressed. Electronic address: myqiang@nju.edu.cn.

$$\frac{NF}{\rho_0 k_B T V} = -\bar{\varphi}_{br}\ln\left(\frac{Q_{br}}{V\bar{\varphi}_{br}}\right) - \bar{\varphi}_{co}\ln\left(\frac{Q_{co}}{V\bar{\varphi}_{co}}\right) - \bar{\varphi}_s N\ln\left(\frac{Q_s}{V\bar{\varphi}_s}\right) + \frac{1}{V}\int d\mathbf{r}\{\chi_{AB}N[\varphi_{br}(\mathbf{r})+\varphi_A(\mathbf{r})]\varphi_B(\mathbf{r}) + \chi_{AS}N[\varphi_A(\mathbf{r})+\varphi_{br}(\mathbf{r})]\varphi_s(\mathbf{r}) + \chi_{BS}N\varphi_B(\mathbf{r})\varphi_s(\mathbf{r}) - W_s(\mathbf{r})\varphi_s(\mathbf{r}) - W_{br}(\mathbf{r})\varphi_{br}(\mathbf{r}) - W_A(\mathbf{r})\varphi_A(\mathbf{r}) - W_B(\mathbf{r})\varphi_B(\mathbf{r}) - \xi(\mathbf{r})[1-\varphi_{br}(\mathbf{r})-\varphi_A(\mathbf{r})-\varphi_B(\mathbf{r}) - \varphi_s(\mathbf{r})]\}, \quad (1)$$

where k_B is the Boltzmann constant and T is the temperature. χ_{AB}, χ_{AS}, and χ_{BS} are the Flory interaction parameters between A-B monomers, A-monomer–solvent, and B-monomer–solvent, respectively. $\varphi_{br}(\mathbf{r})$ is the local volume fraction of grafted chains, $\varphi_s(\mathbf{r})$ is the local volume fraction of solvent, $\varphi_A(\mathbf{r})$ and $\varphi_B(\mathbf{r})$ are the local volume fractions of A and B segments, and $\xi(\mathbf{r})$ is the potential field that ensures the incompressibility of the system. $W_{br}(\mathbf{r})$ is the self-consistent field felt by grafted polymer, $W_s(\mathbf{r})$ is the self-consistent field felt by solvent, and $W_A(\mathbf{r})$ and $W_B(\mathbf{r})$ are the self-consistent fields felt by A and B segments of copolymers. $Q_{br}=\int d\mathbf{r}q_1(\mathbf{r},s)q_1^{\dagger}(\mathbf{r},s)$ and $Q_{co}=\int d\mathbf{r}q_2(\mathbf{r},s)q_2^{\dagger}(\mathbf{r},s)$ are single-chain partition functions for brushes and copolymers, respectively. $Q_s=\int d\mathbf{r}q_s(\mathbf{r},1/N)$ is a solvent partition function in the external field $W_s(\mathbf{r})$. The end-segment distribution functions $q_i(\mathbf{r},s)$ and $q_i^{\dagger}(\mathbf{r},s)$ represent the probability of finding monomers at position $\mathbf{r}$, respectively, from two distinct ends of chains, which satisfy the modified diffusion equations

$$\frac{\partial q_i}{\partial s} = \frac{a^2N}{6}\nabla^2 q_i - W_i(\mathbf{r})q_i \quad (2)$$

and

$$\frac{\partial q_i^{\dagger}}{\partial s} = -\frac{a^2N}{6}\nabla^2 q_i^{\dagger} + W_i(\mathbf{r})q_i^{\dagger}, \quad (3)$$

respectively. For the grafted chains in the field $W_{br}(\mathbf{r})$, the initial condition is $q_1(x,z=0 \text{ or } L_z,0)=1$, $q_1(x,z\neq 0 \text{ or } L_z,0)=0$, and $q_1^{\dagger}(x,z,1)=1$, which means that the end of brush chains can move on the substrates, although the total number of chains on surfaces is fixed. These have been called liquid brushes, in contrast to solid brushes where the immobile chains are anchored onto the surfaces [37]. Here we consider the liquid brush case because of its wide-ranging applications in colloidal and biological systems and, at the same time, for computational efficiency. Furthermore, compared with immobile cases, we find that no distinct deviation is found under long and densely grafted homogeneous chains [36]. For copolymer chains in the fields $W_A(\mathbf{r})$ $(0\leqslant s\leqslant f_A$ along the A block) and $W_B(\mathbf{r})$ $(f_A<s\leqslant 1$ along the B block), the initial conditions are $q_2(x,z,0)=1$ and $q_2^{\dagger}(x,z,1)=1$, respectively. In addition, the only allowed trajectory of polymer chains is within the region $0\leqslant z\leqslant L_z$. For small-molecule solvent, the modified diffusion equation becomes [27]

$$\frac{\partial q_s}{\partial s} = -W_s q_s. \quad (4)$$

By minimizing the free energy in Eq. (1) with respect to $W_{br}(\mathbf{r})$, $W_A(\mathbf{r})$, $W_B(\mathbf{r})$, $W_s(\mathbf{r})$, $\varphi_{br}(\mathbf{r})$, $\varphi_A(\mathbf{r})$, $\varphi_B(\mathbf{r})$, $\varphi_s(\mathbf{r})$, and $\xi(\mathbf{r})$, we obtain a set of self-consistent equations that describe the equilibrium morphology of confined copolymer solution,

$$W_{br}(\mathbf{r}) = \chi_{AB}N\varphi_B + \chi_{AS}N\varphi_s + \xi(\mathbf{r}), \quad (5)$$

$$W_A(\mathbf{r}) = \chi_{AB}N\varphi_B + \chi_{AS}N\varphi_s + \xi(\mathbf{r}), \quad (6)$$

$$W_B(\mathbf{r}) = \chi_{AB}N(\varphi_{br}+\varphi_A) + \chi_{BS}N\varphi_s + \xi(\mathbf{r}), \quad (7)$$

$$W_s(\mathbf{r}) = \chi_{AS}N(\varphi_{br}+\varphi_A) + \chi_{BS}N\varphi_B + \xi(\mathbf{r}), \quad (8)$$

$$\varphi_{br}(\mathbf{r}) = \frac{\bar{\varphi}_{br}V}{Q_{br}}\int_0^1 dsq_1(\mathbf{r},s)q_1^{\dagger}(\mathbf{r},s), \quad (9)$$

$$\varphi_A(\mathbf{r}) = \frac{\bar{\varphi}_{co}V}{Q_{co}}\int_0^{f_A} dsq_2(\mathbf{r},s)q_2^{\dagger}(\mathbf{r},s), \quad (10)$$

$$\varphi_B(\mathbf{r}) = \frac{\bar{\varphi}_{co}V}{Q_{co}}\int_{f_A}^1 dsq_2(\mathbf{r},s)q_2^{\dagger}(\mathbf{r},s), \quad (11)$$

$$\varphi_s(\mathbf{r}) = \frac{\bar{\varphi}_s V}{Q_s}q_s\left(\mathbf{r},\frac{1}{N}\right), \quad (12)$$

$$\varphi_{br}+\varphi_A+\varphi_B+\varphi_s = 1. \quad (13)$$

Our actual implementation of the SCFT follows the real-space combinatorial screening algorithm of Drolet and Fredrickson [38] to numerically solve the self-consistent equations. To search the stable phases of the film, we first ascertain the symmetries of the cylinder or lamellar structural formation, and then calculate the free energy of the film. Furthermore, the total free-energy minimization of the system with respect to the selected simulation sizes is required by adjusting the lateral dimension [39]. All the sizes are in units of a.

We first study the effects of copolymer solution concentration on the equilibrium morphologies of the present system confined between two homopolymer-grafted substrates. Here, we will choose $\chi_{AB}N=20$ and $\chi_{AS}N=\chi_{BS}N=0$ (i.e., the solvent molecules are neutral to A/B copolymer components, and there are no interactions between solvent and copolymer components), and other parameters are fixed to be $f_A=0.67$ and $\sigma=0.2$. In Fig. 1, snapshots of the left-hand side show the reentrant hexagonal→lamellar→hexagonal phase transition for asymmetric copolymer solution films with the dilution of copolymer solution. On the right-hand side of Fig. 1, the corresponding density profiles for the brush (φ_{br}), solvent (φ_s), copolymer (φ_{co}), and A blocks (φ_A) and B blocks (φ_B) are given along the z axis. A set of curves for different solution concentrations ψ_{co} has similar shapes. The periodical variation of relative concentrations φ_A and φ_B of copolymer

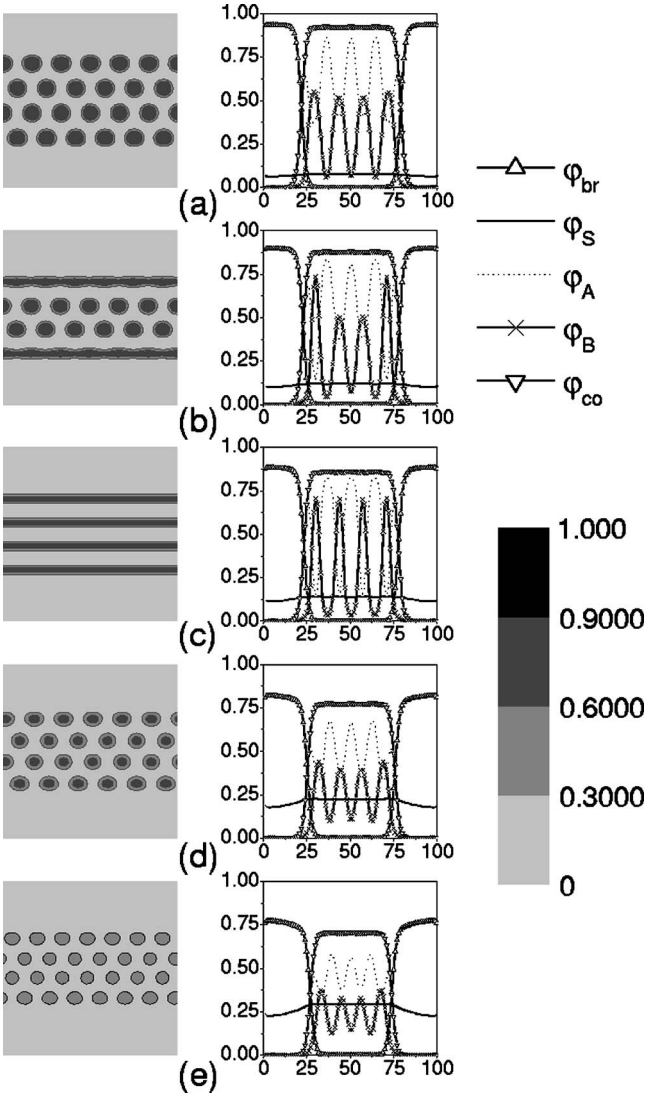

FIG. 1. The density distributions (left column) for the B block of asymmetric A-B copolymer solution at the x-z plane and the corresponding x-direction-averaged profiles (right column) of φ_{br}, φ_s, φ_A, φ_B, and φ_{co} along the z axis. Here, $L_x \times L_z = 100 \times 100$. The gray scale bar shows the local density values of B blocks (left-hand side). (a) $\psi_{co}=0.88$, (b) $\psi_{co}=0.81$, (c) $\psi_{co}=0.78$, (d) $\psi_{co}=0.65$, and (e) $\psi_{co}=0.55$.

components displays the formation of modulated structures of A- and B-block copolymer solutions in confinement. Interestingly, we find that the concentrations φ_A and φ_B of copolymer components remain zero in the region of polymer brushes, while the solvent concentration φ_s has almost the same value at the brush region as in copolymer solution. This means that small-molecule solvents can penetrate into brushes, while long and flexible copolymer chains are excluded out of brushes. This, at the same time, will lead to the relative increase of the copolymer concentration in the region between two brush surfaces, in contrast to that of copolymer solution films confined between hard walls.

As we know, for asymmetric copolymer melts, the bulk phase-separated states are always hexagonal structures. On the other hand, polymer brushes are strongly stretched and

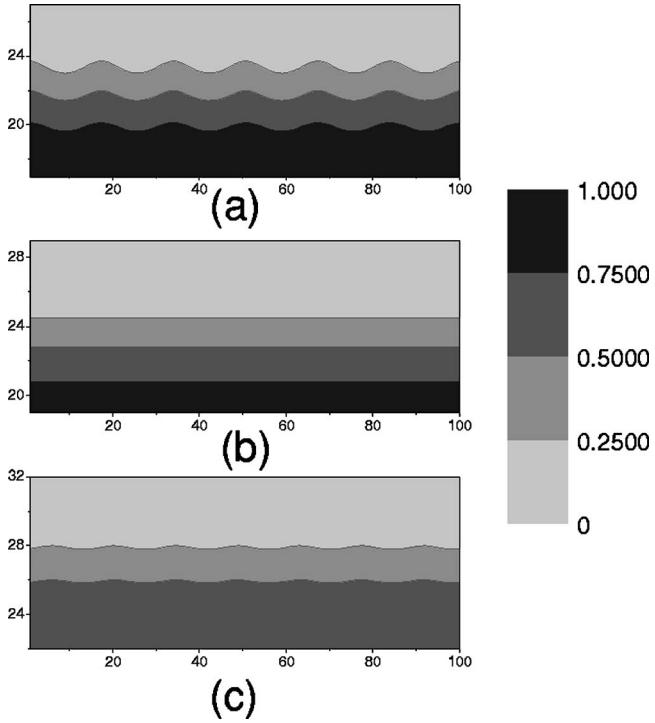

FIG. 2. Density distributions for polymer brushes. (a) $\psi_{co}=0.88$, (b) $\psi_{co}=0.78$, and (c) $\psi_{co}=0.65$.

prefer to form flat interfaces [40]. Therefore, a lamellar phase may be formed under confinement, due to the wetting effect of brush-formed surface to the A block of the copolymer. These two factors compete with each other in the confined film and may result in the formation of final structures of copolymer solution. When the concentration of asymmetric copolymer solution is high, a strong repulsive interaction of A and B segments ($\propto \psi_{co}\chi_{AB}N$) will lead to large interface tension between A and B domains, which tends to drive the formation of hexagonally arranged cylinder phases [see Fig. 1(a)]. Instead, the brush-formed interface will be deformed to maintain bulk hexagonal phases of copolymers. Figure 2(a) shows the deformed shape of the brush surface for $\psi_{co}=0.88$, while the brush-formed interface energy is disfavored. In contrast to the hard-wall case, the flexible brush-formed interfaces are soft and can deviate from the flat shape in order to match the formation of different microstructures of the film under the total free-energy minimization of the system. Therefore, such a grafting interface may help to retain the bulk phase behavior of asymmetric copolymer films, and the possible frustrated states due to the confinement between two solid walls can be effectively eliminated by the elastic "soft" grafting interfaces. With increasing the concentration of solvent molecules, the interaction between A and B segments is weakened due to the aggregation of more solvent molecules onto the A/B interfaces [41]. Thus the domains closing to brush interfaces tend to form lamellae due to the wetting effects of brushes, though cylindrical structures are still retained at the middle region. In this case, the brush interface retains flat, as shown in Fig. 2(b), and block A segregates to brush surfaces due to wetting effects. A further increase of solvent will greatly decrease the

A/B interfacial tension. When the confined film thickness conforms to the four-layer thickness of lamellar structure, the system forms a four-layered lamellar phase parallel to the surfaces [see Fig. 1(c)]. The formation of a four-layered lamellar phase favors the conformational entropy of brushes, but the A-B interfacial energy of copolymers is disfavored. When the solvent concentration is sufficiently high, the brush wetting and confinement effects are greatly weakened due to more solvent molecules aggregated at brush interfaces, and the system can be taken as a free asymmetric copolymer film. Interestingly, contrary to a diluted asymmetric copolymer solution confined between the wetting hard walls where the bulk phase structure shows a disordered one for $\psi_{co} \leqslant 0.66$, our system still phase-separates into a hexagonally arranged cylinder structure. This is due to the fact that when the system is confined between polymer brushes, small-molecule solvents can penetrate into brushes, while long and flexible copolymer chains are expelled from brushes (see the concentration profiles of solvent and copolymer components on the right-hand side of Fig. 1). Therefore the copolymer solution film is effectively purified due to the entropy effects of brushes, leading to the possible formation of four-layered cylinder structure [Fig. 1(d)]. However, the formed structure is a weak phase-separated one due to lower A/B interfacial tensions. Figure 2(c) shows the deformed shape of the brush surface in this condition, which tends to become flat with the occurrence of more solvent molecules. Further, Fig. 1(e) also shows such a morphological property when the copolymer solution concentration is 0.55, and even the phase separation may be stopped; instead, a disordered phase is formed.

To clarify the interfacial energetic effects of polymer brushes on the formation of lamellar structures, we calculate the interfacial energy F_{int} of polymer-grafted surfaces, which come from the unfavorable contacts between grafted chains and B component of copolymers. The interfacial energy F_{int} is given by

$$\frac{F_{int}}{k_B T} = \frac{\rho_0}{N} \int d\mathbf{r} \chi_{AB} N \varphi_{br} \varphi_B. \tag{14}$$

Figure 3 shows the interfacial energy of brush-formed surfaces as a function of the copolymer concentration. With decreasing the concentration of solution, the brush-formed surface energy goes down. However, an abrupt reduction of $F_{int}/k_B T$ at the transition point T_1 occurs with the formation of lamellar structures close to the brush interfaces, indicating a preference for a horizontal interface imposed by the brush. As ψ_{co} is reduced to 0.72, the brush-formed interfacial energy is increased, due to the formation of cylinder structures.

Furthermore, by calculating the A-block entropy S_A/k_B and B-block entropy S_B/k_B per copolymer chain,

$$\frac{S_A}{k_B} = \frac{1}{V} \int [\rho(\mathbf{r}) \ln q_2(\mathbf{r}, f_A) + W_A(\mathbf{r}) \varphi_A(\mathbf{r})] d\mathbf{r}, \tag{15}$$

$$\frac{S_B}{k_B} = \frac{1}{V} \int [\rho(\mathbf{r}) \ln q_2^{\dagger}(\mathbf{r}, f_A) + W_B(\mathbf{r}) \varphi_B(\mathbf{r})] d\mathbf{r}, \tag{16}$$

with

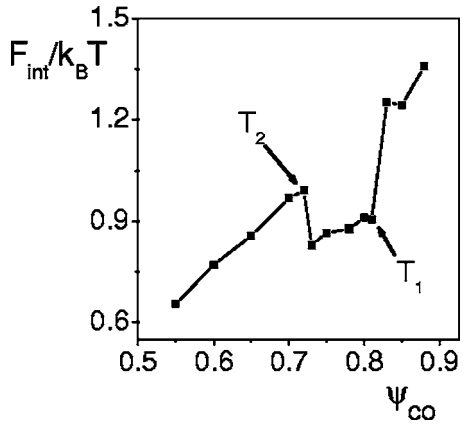

FIG. 3. The interfacial energy of brush-formed surfaces as a function of copolymer concentration ψ_{co}. T_1 indicates the formation of lamellar structures close to the brush interfaces, and T_2 denotes the reentrant transition to hexagonal phases with the decrease of the copolymer concentration ψ_{co}.

$$\rho(\mathbf{r}) = \frac{\bar{\varphi}_{co} V}{Q_{co}} q_2(\mathbf{r}, s) q_2^{\dagger}(\mathbf{r}, s), \tag{17}$$

we obtain respective A-block entropy S_A/k_B and B-block entropy S_B/k_B per copolymer chain as a function of copolymer concentration, as shown in Fig. 4. Generally, S_A/k_B increases with the dilution of copolymer solution due to more available configurational space, but for the minority component B of copolymer, S_B/k_B changes slightly. For the middle concentrations of copolymer solution, however, the relative large changes due to the entropic win and loss, which show the A-B-block chain stretching and compressing behaviors, occur with the formation of lamellar structures. When the lamellar structure begins to form, the B-block chain stretches and its entropy will become small, whereas the A-block entropy will become relatively large.

We now calculate the entropy of a grafted polymer, S_{br}/k_B, which is given by [42]

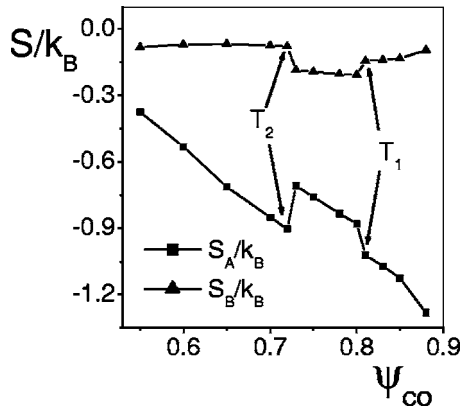

FIG. 4. A-block entropy S_A/k_B and B-block entropy S_B/k_B per copolymer chain as a function of the copolymer concentration ψ_{co}. T_1 indicates the formation of lamellar structures close to the brush interfaces, and T_2 denotes the reentrant transition to hexagonal phases with the decrease of the copolymer concentration ψ_{co}.

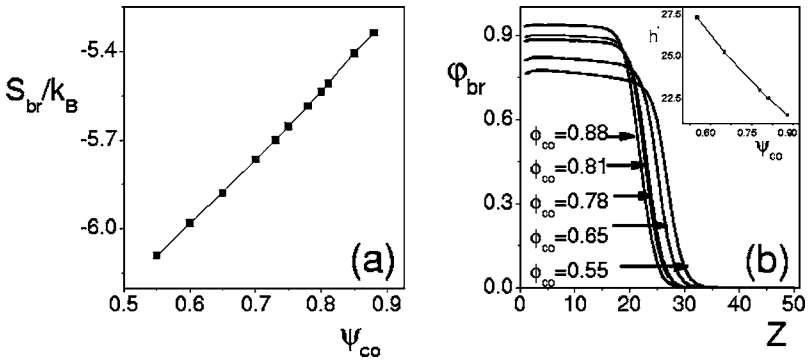

FIG. 5. (a) A grafted-chain entropy (S_{br}/k_B) as a function of copolymer concentration. (b) Density profiles of polymer brushes with different copolymer concentrations. The inset shows the thickness of polymer brushes as a function of ψ_{co}.

$$\frac{S_{br}}{k_B} = \frac{\rho_0 V}{N n_{br}} \left[\bar{\varphi}_{br} \ln\left(\frac{Q_{br}}{V \bar{\varphi}_{br}} \right) + \frac{1}{V} \int W_{br} \varphi_{br} d\mathbf{r} \right]. \quad (18)$$

Figure 5(a) shows the entropy of a grafted chain, S_{br}/k_B, as a function of copolymer concentration. We find on decreasing the copolymer concentration, S_{br}/k_B decreases rapidly, meaning that the entropy penalty of brushes becomes more severe with increasing the solvent density. This is due to the penetration of solvent molecules into the region of brushes where the movement of grafted chains is greatly restricted and the configuration of polymer brushes is largely decreased. Figure 5(b) shows one-dimensional density profiles of polymer brushes beginning from one of the substrates for different copolymer concentrations $\psi_{co}=0.88$, $\psi_{co}=0.81$, $\psi_{co}=0.78$, $\psi_{co}=0.65$, and $\psi_{co}=0.55$. It is well known that the height of a dry brush satisfies $h=\sigma N/\rho_0$ in the incompressible system of brush and homopolymer molecules [43]. However, due to the existence of small-molecule solvent distributed in the whole film, the formula of the brush height should be revised as $h'=\sigma N/\rho_0 \varphi_{br} \simeq \sigma N/\rho_0[1-(1-\bar{\varphi}_{br})(1-\psi_{co})]$. As the copolymer concentration is decreased, the brush height h' increases as a result of more solvent molecules entering the brush region, which is shown in the inset of Fig. 5(b). The effective thickness of film can be defined by subtracting the brush height from the distance L_z between two substrates—i.e., $d_{eff}=L_z-2h'$. Thus, we can conclude that the effective thickness d_{eff} of the film is changeable and decreases with decreasing the concentration of solution. When ψ_{co} is between 0.72 and 0.8, the four-layered lamellar structure appears and the lamellar thickness is around 13.5. Such a lamellar structure can be realized by adjusting the film thickness via varying the solution concentration, which cannot be achieved in the case of hard-wall confinement.

To analyze the stability of the formed ordering phases, we undertake the free-energy calculations by taking hexagonal, lamellar, and hexagonal-lamellar mixed states as the initial configurations, respectively. The method is similar to that performed in some similar systems [2,4,10]. We find that for $\psi_{co}<0.72$, the final ordering structure is always hexagonal no matter what the initial configuration is. For $\psi_{co}>0.72$, on the other hand, Fig. 6 shows the difference $\Delta F=N(F_l-F_h)/\rho_0 k_B T V$ between the free energy in the lamellar (F_l) and the hexagonal (F_h) phases. We find $F_l<F_h$ in the range $\psi_{co}=0.72-0.8$, implying that the stable phases are lamellae. For $\psi_{co}>0.82$ where $F_h<F_l$, the final stable phase becomes hexagonal. When ψ_{co} is between 0.80 and 0.82, by comparing the free energies of different ordering structures, we find that the free energy of the mixed hexagonal-lamellar structure is the smallest, although the difference is slight, and thus the stable morphology will be the hexagonal-lamellar mixed structure. Furthermore, based on the above analysis which exhibited the symmetries of the cylinder, lamellar, and hexagonal-lamellar mixed structures, we can minimize the free energy of the system by adjusting the lateral dimension to search the phase boundaries between the different ordering phases. A complete phase diagram as a function of the incompatibility parameter $\chi_{AB}N$ and the copolymer concentration ψ_{co} is shown in Fig. 7. The occurrence of regions of stability for the distinct ordering phases signifies the competition of the wetting effect of brush-formed surfaces and the bulk phase behavior of asymmetric copolymer driven by the *A*-*B* interfacial tension. For $\chi_{AB}N<19$, there is the only hexagonal ordering structure because the wetting effect due to the small $\chi_{AB}N$ cannot drive the formation of the lamellar structures. When the incompatibility parameter $\chi_{AB}N$ is relatively large, even a double reentrant transition occurs with the decrease of the copolymer concentration ψ_{co}, indicating that the significant competition still exists even for diluted copolymer solutions. Further increase of the incompatibility parameter $\chi_{AB}N$ enlarges the region of mixed hexagonal-lamellar phases. This is due to the competition between the strong wetting effect driving the formation of lamellar structure close to brush surfaces and

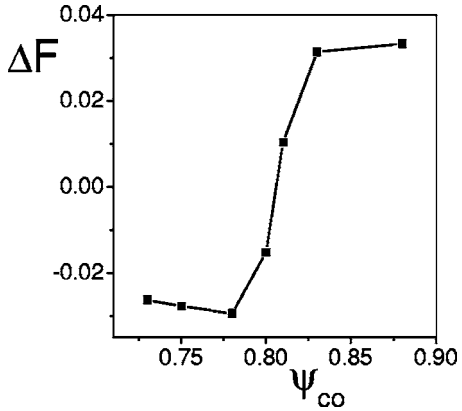

FIG. 6. The free-energy difference $\Delta F=N(F_l-F_h)/\rho_0 k_B T V$ for the lamellar phase (F_l) and the hexagonal phase (F_h) upon varying the copolymer concentration ψ_{co}.

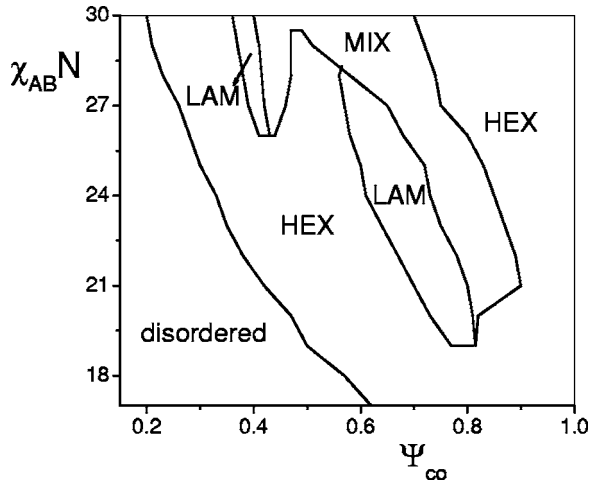

FIG. 7. Phase diagram of the confined asymmetric copolymer solution film as functions of $\chi_{AB}N$ and ψ_{co}. Here, $\chi_{AS}N=\chi_{BS}N=0$, $f_A=0.67$, and $\sigma=0.2$. The ordered phases are labeled as HEX (hexagonal), LAM (lamellar), and MIX (hexagonal-lamellar mixed phase).

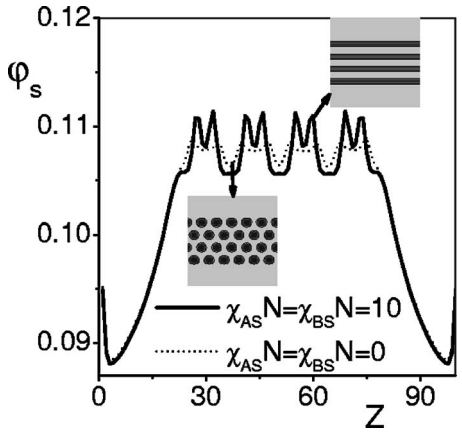

FIG. 8. One-dimensional density profiles of solvent with two different interactions between solvents and A/B segments. The inset patterns show hexagonal and lamellar structures of copolymer solutions, respectively corresponding to the interactions $\chi_{AS}N=\chi_{BS}N=0$ and $\chi_{AS}N=\chi_{BS}N=10$.

strong phase separation of asymmetric copolymers favoring the bulk hexagonal phase at the middle region.

Finally, to examine the effects of the solvent distribution on the morphological transition between hexagonal and lamellar phases of copolymer solutions, we increase the interaction between solvent and segments, while the solvent molecules are still neutral to A/B copolymer components. Figure 8 shows the solvent profiles along the z direction for the cases $\chi_{AS}N=\chi_{BS}N=0$ and $\chi_{AS}N=\chi_{BS}N=10.0$ when $\chi_{AB}N=20$ and $\psi_{co}=0.83$. For the repulsive interaction between segments and solvent, more solvent molecules are expelled from polymer components and aggregate onto the interface of A/B domains, which screens unfavorable A-B block contacts. Such a behavior of solvent leads to the decrease of interface energy between A and B monomers, which thus strengthens the trend of the phase transition from hexagonal to lamellar due to the wetting effect of brush-formed surfaces. We can clearly see from Fig. 8 that with the increase of the interaction between solvent and segments, a phase transition from hexagonal to lamellar structures appears.

In summary, we have investigated the effects of the solvent on the equilibrium morphologies of asymmetric copolymer solution films confined between two polymer-coated surfaces. With the decrease of the concentration of copolymer solution films, a reentrant structure transformation between hexagonal-lamellar-hexagonal phases is observed, due to the competition between the wetting effect of brush-formed surface and the bulk phase behavior of asymmetric copolymer driven by the A-B interfacial tension. We conclude that for higher and lower copolymer solution concentrations, the formation of hexagonal structures is attributed to the bulk phase behavior of asymmetric copolymer driven by the A/B interfacial tension, while the lamellar phase for the middle copolymer concentration appears as a result of the wetting effects of the brush-formed interface under a conformable film thickness. A phase diagram displaying the hexagonal, lamellar, and mixed hexagonal-lamellar phases is revealed, and the result may provide a simple and helpful guide for fabricating functionally useful microstructures of phase-separated copolymer solutions by introducing polymer-grafted "soft" walls. Finally, we should point out that in the present SCFT, the composition fluctuation [44,45] is neglected. Recently, Laradji *et al.* [46] developed a theory for anisotropic fluctuations in ordered phases of diblock copolymer melts by means of a self-consistent expansion around the exact mean-field solution. It will be a further challenging problem to extend their approach to account for composition fluctuations of confined copolymer films in the presence of diluting solvents. This work is in progress.

This work was supported by the National Natural Science Foundation of China, Grant Nos. 10334020, 10021001, and 20490220.

[1] F. S. Bates and G. H. Fredrickson, Phys. Today **52**(2), 32 (1999); I. W. Hamley, Nanotechnology **14**, R39 (2003); M. Lazzari and M. A. Lopez-Quintela, Adv. Mater. (Weinheim, Ger.) **15**, 1583 (2003).

[2] M. W. Matsen, J. Chem. Phys. **106**, 7781 (1997).

[3] M. J. Fasolka and A. M. Mayes, Annu. Rev. Mater. Sci. **31**, 323 (2001), and references therein.

[4] G. Pickett and A. C. Balazs, Macromolecules **30**, 3097 (1997); M. J. Fasolka, P. Banerjee, A. M. Mayes, G. Pickett, and A. C. Balazs, *ibid.* **33**, 5702 (2000); J. Y. Lee, Z. Shou, and A. C. Balazs, Phys. Rev. Lett. **91**, 136103 (2003).

[5] P. Lambooy, T. P. Russell, G. J. Kellogg, A. M. Mayes, P. D. Gallagher, and S. K. Satija, Phys. Rev. Lett. **72**, 2899 (1994).

[6] N. Koneripalli, N. Singh, R. Levicky, F. S. Bates, P. D. Gal-

lagher, and S. K. Satija, Macromolecules **28**, 2897 (1995).
[7] M. S. Turner, M. Rubinstein, and M. Marques, Macromolecules **27**, 4986 (1994).
[8] D. G. Walton, G. J. Kellogg, A. M. Mayes, P. Lambooy, and T. P. Russell, Macromolecules **27**, 6225 (1994); C. Harrison *et al.*, *ibid.* **33**, 857 (2000); H. C. Kim and T. P. Russell, J. Polym. Sci., Part A: Polym. Chem. **39**, 663 (2001).
[9] A. K. Chakraborty and A. J. Golumbfskie, Annu. Rev. Phys. Chem. **52**, 537 (2001).
[10] T. Geisinger, M. Muller, and K. Binder, J. Chem. Phys. **111**, 5241 (1999).
[11] D. Petera and M. Muthukumar, J. Chem. Phys. **109**, 5101 (1998).
[12] T. Thurn-Albrecht, J. Schotter, A. Kästle, N. Emley, T. Shibauchi, L. Krusin-Elbaum, K. Guarini, C. T. Black, M. T. Tuominen, and T. P. Russell, Science **290**, 2126 (2000).
[13] T. Thurn-Albrecht, R. Steiner, J. DeRouchey, C. M. Stafford, E. Huang, M. Ball, M. T. Tuominen, C. J. Hawker, and T. P. Russell, Adv. Mater. (Weinheim, Ger.) **12**, 787 (2000).
[14] G. Kim and M. Libera, Macromolecules **31**, 2670 (1998).
[15] S. H. Kim, M. J. Misner, T. Xu, M. Kimura, and T. P. Russell, Adv. Mater. (Weinheim, Ger.) **16**, 226 (2004).
[16] L. Rockford, Y. Liu, P. Mansky, T. P. Russell, M. Yoon, and S. G. J. Mochrie, Phys. Rev. Lett. **82**, 2602 (1999).
[17] S. O. Kim, H. H. Solak, H. Stoykovich, N. J. Ferrie, J. J. de Pablo, and P. F. Nealey, Nature (London) **424**, 411 (2003).
[18] M. J. Fasolka, D. J. Harris, A. M. Mayes, M. Yoon, and S. G. J. Mochrie, Phys. Rev. Lett. **79**, 3018 (1997).
[19] E. Sivaniah, Y. Hayashi, M. Iino, T. Hahimoto, and K. Fukunaga, Macromolecules **36**, 5894 (2003).
[20] S. H. Anastasiadis, T. P. Russell, S. K. Satija, and C. F. Majkrzak, Phys. Rev. Lett. **62**, 1852 (1989).
[21] T. P. Russell, G. Coulon, V. R. Deline, and D. C. Miller, Macromolecules **22**, 4600 (1989).
[22] P. Mansky, Y. Liu, E. Huang, T. P. Russell, and C. J. Hawker, Science **275**, 1458 (1997).
[23] E. Huang, L. Rockford, T. P. Russell, C. J. Hawker, and J. Mays, Nature (London) **395**, 757 (1998).
[24] G. Brown and A. Chakrabarti, J. Chem. Phys. **102**, 1440 (1995).
[25] Q. Wang, P. E. Nealey, and J. J. de Pablo, Macromolecules **36**, 1731 (2003).
[26] E. Helfand and Y. Tagami, J. Chem. Phys. **56**, 3592 (1972).
[27] C.-I. Huang and T. P. Lodeg, Macromolecules **31**, 3556 (1998).
[28] G. H. Fredrickson and L. Leibler, Macromolecules **22**, 1238 (1989).
[29] J. Noolandi and K. M. Hong, Ferroelectrics **30**, 117 (1980).
[30] K. M. Hong and J. Noolandi, Macromolecules **16**, 1083 (1983).
[31] T. P. Lodge, C. Pan, X. Jin, Z. Liu, J. Zhao, W. W. Maurer, and F. S. Bates, J. Polym. Sci., Part B: Polym. Phys. **33**, 2289 (1995).
[32] T. P. Lodge, M. W. Hamersky, K. J. Hanley, and C.-I. Huang, Macromolecules **30**, 6139 (1997).
[33] M. W. Matsen and M. Schick, Phys. Rev. Lett. **72**, 2660 (1994).
[34] S. T. Milner, Science **251**, 905 (1991).
[35] G. J. Fleer, M. A. C. Stuart, J. M. H. M. Scheutjens, T. Cosgrove, and B. Vincent, *Polymers at Interfaces* (Chapman and Hall, London, 1993); M. W. Matsen and J. M. Gardiner, J. Chem. Phys. **115**, 2794 (2001).
[36] C. L. Ren, K. Chen, and Y. Q. Ma, J. Chem. Phys. **122**, 154904 (2005).
[37] G. Subramanian, D. R. M. Williams, and P. A. Pincus, Macromolecules **29**, 4045 (1996).
[38] F. Drolet and G. H. Fredrickson, Phys. Rev. Lett. **83**, 4317 (1999); Macromolecules **34**, 5317 (2001).
[39] Y. Bohbot-Raviv and Z. G. Wang, Phys. Rev. Lett. **85**, 3428 (2000).
[40] There exists an interface between the copolymer solution and brushes, while polymer brushes are composed of the same monomers as the *A*-type component of copolymers; see, for example, A. V. Ruzette and L. Leibler, Nat. Mater. **4**, 19 (2005).
[41] Y. C. Lin, M. Müller, and K. Binder, J. Chem. Phys. **121**, 3816 (2004).
[42] M. W. Matsen and F. S. Bates, J. Chem. Phys. **106**, 2436 (1997); P. Maniadis, R. B. Thompson, K. O. Rasmussen, and T. Lookman, Phys. Rev. E **69**, 031801 (2004).
[43] M. W. Matsen, J. Chem. Phys. **122**, 144904 (2005).
[44] G. H. Fredrickson and E. Helfand, J. Chem. Phys. **87**, 697 (1987).
[45] A. N. Semenov, Macromolecules **22**, 2849 (1989); S. A. Brasovskii, Zh. Eksp. Teor. Fiz. **68**, 175 (1975) [Sov. Phys. JETP **41**, 85 (1975)]; L. Leibler, Macromolecules **13**, 1602 (1980).
[46] M. Laradji, A. C. Shi, J. Noolandi, and R. C. Desai, Macromolecules **30**, 3242 (1997).